Pharmaceutical Research, Vol. 12, No. 6, 1995

Research Article

Human Insulin Receptor Monoclonal Antibody Undergoes High Affinity Binding to Human Brain Capillaries in Vitro and Rapid Transcytosis Through the Blood–Brain Barrier in Vivo in the Primate

William M. Pardridge,[1,2] Young-Sook Kang,[1] Jody L. Buciak,[1] and Jing Yang[1]

Received December 12, 1994; accepted February 2, 1995

Purpose. The ability of monoclonal antibodies against the human insulin receptor to undergo transcytosis through the blood-brain barrier (BBB) was examined in the present studies. ***Methods.*** Two murine monoclonal antibodies (MAb83-7 and MAb83-14) which bind different epitopes within the α-subunit of the human insulin receptor were examined using isolated human brain capillaries, frozen sections of primate brain, and in vivo pharmacokinetic studies in anesthetized Rhesus monkeys. ***Results.*** Both antibodies strongly illuminated capillary endothelium in immunocytochemical analysis of frozen sections of brain from Rhesus monkey but not squirrel monkey. Both monoclonal antibodies, in the iodinated forms, bound to human brain microvessels, although the binding and endocytosis of MAb83-14 was approximately 10-fold greater than MAb83-7. The active binding of MAb83-14 to the human insulin receptor was paralleled by a very high rate of transport of this antibody through the BBB in vivo in two anesthetized Rhesus monkeys. The BBB permeability-surface area (PS) product in neocortical gray matter was 5.4 ± 0.6 μL/min/g, which is severalfold greater than previous estimates of the PS product for receptor-specific monoclonal antibody transport through the BBB. The brain delivery of MAb83-14 to the Rhesus monkey brain was high and 3.8 ± 0.4% of the injected dose was delivered to 100 g of brain at 3 hours after a single intravenous injection. In contrast, there was no brain uptake of the mouse IgG_{2a} isotype control antibody. ***Conclusions.*** These studies demonstrate an unexpected high degree of transcytosis of a monoclonal antibody through the primate BBB in vivo.

KEY WORDS: blood–brain barrier; BBB; transcytosis; insulin receptor; drug delivery.

INTRODUCTION

The delivery of therapeutics to the brain is impeded by the presence of the brain capillary endothelial wall, which makes up the blood-brain barrier (BBB) in vivo. The BBB is formed by epithelial-like tight junctions within the capillary endothelia of vertebrate brain (1), and these junctions preclude the free diffusion of therapeutics from blood to brain interstitial space. One physiological-based strategy for drug delivery through the BBB is the use of chimeric peptides (2). The latter are comprised of conjugates of a drug, that is normally not transported through the BBB, and a brain drug delivery vector. Vectors are modified proteins or antibodies that undergo absorptive-mediated or receptor-mediated transcytosis through the BBB. The model vector for absorptive-mediated transcytosis is cationized albumin (3), and the model vector for receptor-mediated transcytosis is the OX26 murine monoclonal antibody to the rat transferrin receptor (4,5). Previous studies have shown in vivo CNS pharmacologic effects following coupling of drug to the OX26 monoclonal antibody (6,7). The OX26 monoclonal antibody binds the BBB transferrin receptor (8), which mediates the transcytosis through the BBB of transferrin (9,10), and gains access to brain interstitial space via this pathway. The OX26 monoclonal antibody is specific to the rat receptor (8,11), and it would be advantageous to develop a brain drug delivery vector that can be used in humans. A human-specific BBB transport vector may also be active at the primate BBB, and this would allow for in vivo testing of the vector in an animal model.

Potential candidates for human brain drug delivery vectors are monoclonal antibodies against receptors present on brain capillary endothelium. Previous studies have shown high concentrations of the insulin receptor on the BBB (12), and this receptor mediates the transcytosis of circulating insulin from blood to brain interstitial fluid (13). Therefore, the present investigations examine two different murine monoclonal antibodies to the human insulin receptor with respect to the ability of these antibodies to undergo transport through the BBB. Isolated autopsy human brain capillaries are used as an in vitro model system of antibody binding and

[1] Department of Medicine and Brain Research Institute, UCLA School of Medicine, Los Angeles, California 90024.

[2] To whom correspondence should be addressed at Department of Medicine, UCLA School of Medicine, Los Angeles, California 90024-1682.

0724-8741/95/0600-0807$07.50/0

endocytosis at the human BBB, and the in vivo transcytosis through the primate BBB is examined in the anesthetized Rhesus monkey. The monoclonal antibodies are designated MAb83-7, which binds an epitope within amino acids 191-297 of the α-subunit of the human insulin receptor, and MAb83-14, which binds an epitope within amino acids 469-592 of the α-subunit of the human insulin receptor (14). Both anitbodies bind epitopes that are accessible in the native state of the receptor (15).

MATERIALS AND METHODS

Materials

MAb83-7 and MAb83-14 mouse ascites were provided by Professor Kenneth Siddle (Department of Clinical Biochemistry, University of Cambridge). Frozen brain from two Rhesus monkeys (21 year old female, 20 year old male) and one squirrel monkey (21 years old) was provided by Dr. Lary Walker (Neuropathology Lab, Johns Hopkins School of Medicine). ^{3}H-N-succinimidylpropionate (NSP), 102 Ci/mmol, and ^{125}I-iodine were obtained from Amersham Corp. (Arlington Heights, IL). Mouse IgG1 and mouse IgG_{2a} were purchased from Cappel (West Chester, PA). Chloramine T was from MCB Reagents (Cincinnati, OH). Protein G-Sepharose 4 Fast Flow was obtained from Pharmacia (Piscataway, NJ). Vectastain ABC-Elite reagents were obtained from Vector Laboratories (Burlingame, CA). Two 20 year old female Rhesus monkeys were purchased from Buckshire Corp. (Perkasie, PA) weighing 6.8 kg (designated RM1) and 8.0 kg (designated RM2). Microvessels were isolated from 3 different human autopsy brains obtained from Dr. Harry Vinters of the Division of Neuropathology, Department of Pathology, UCLA Medical Center. The post-mortem internal (PMI) varied from 6 to 31 hours, which is within the PMI of brains obtained for assaying the human BBB insulin receptor (12). Porcine insulin and all other reagents were obtained from Sigma Chemical Corp. (St. Louis, MO). O.C.T. (optimal cutting temperature) embedding medium for frozen tissue specimens was purchased from Miles, Inc. (Elkhart, IN).

Monoclonal Antibody Purification and Radiolabeling

The MAb83-14 or MAb83-7 were purified from mouse ascites using Protein G-Sepharose 4 Fast Flow affinity chromatography, as described previously (16). The yield of purified monoclonal antibody ranged from 6-9 mg per ml of ascites. Initially, MAb83-7 and MAb83-14 were tritiated by propionylation of lysine residues with ^{3}H-NSP (17). However, initial binding studies with human brain capillaries showed that this radiolabeling procedure eliminated specific binding to the human insulin receptor. Therefore, the MAbs were subsequently radiolabeled with ^{125}I-iodine and chloramine T; 20 μg of monoclonal antibody was iodinated with 2 mCi of ^{125}I-iodine and 4.2 nmol of chloramine T. The iodination reaction was quenched with the addition of 25 nmol of sodium metabisulfite and radiolabeled antibody was purified by Sephadex G25 gel filtration chromatography. The specific activity of the iodinated monoclonal antibody was 39 μCi/μg with a trichloroacetic acid (TCA) precipitability of 99%. Mouse IgG_{2a} was tritiated with ^{3}H-NSP using procedures described previously (17) to a specific activity of 0.35 μCi/μg and a TCA precipitability of 94%. Insulin was iodinated as described previously (12).

Radioreceptor Assays

Binding of ^{125}I-MAb83-14 or MAb83-7 to capillaries isolated from 3 different human autopsy brains was measured as described previously (12). Both total binding and binding resistant to a mild acid wash were determined. Human brain capillaries (equivalent to approximately 100-140 μg protein) were mixed in 0.45 ml of Ringer-Hepes buffer (pH = 7.4) in the presence of 0.20 μCi/ml of ^{125}I-labeled monoclonal antibodies. Various concentrations of unlabeled monoclonal antibody, unlabeled mouse IgG1 or mouse IgG_{2a}, or unlabeled porcine insulin were added to the mixture, and incubation was performed at 37°C for up to 2 hours. Incubation was terminated by centrifugation at 10,000g for 45 seconds. The capillary pellet was solubilized in 1 N NaOH for ^{125}I counting and protein assays as described previously (17).

Capillaries were isolated from 3 different fresh human autopsy brains (designated H1, H2, H3, Table 1) using a mechanical homogenization technique described previously (12). Isolated microvessels were cryo-preserved in 0.25 M sucrose, 0.02 M Tris (pH = 7.4), and 2 mM dithiothreitol, and stored in liquid nitrogen for periods ranging from 1-11 months.

The binding of ^{125}I-insulin to human brain capillaries was measured at 25°C for 90 minutes in the presence of 0 or 10 μg/ml unlabeled insulin, or 0-1 μg/ml unlabeled MAb83-14 or mouse IgG_{2a}, as described previously (12).

Pharmacokinetics and Brain Delivery

Rhesus monkey 1 (RM1) or Rhesus monkey 2 (RM2) were anesthetized with 100 mg of intramuscular ketamine and 0.5-2.0% halothane in the operative suite of the UCLA

Table 1. Uptake of [^{125}I]MAb83-14 by Isolated Human Brain Microvessels[a]

No.	Age/sex	Diagnosis	Incubation time (hours)			
			0.25	0.5	1	2
H1	45/F	lymphoma	149 ± 8	211 ± 13	300 ± 6	386 ± 35
H2	68/M	heart disease	144 ± 11	167 ± 2	243 ± 3	306 ± 8
H3	68/M	respiratory failure	103 ± 5	149 ± 11	156 ± 11	195 ± 5

[a] Mean ± S.E. (n = 3). Data are expressed as % uptake per mg_p of capillaries. Incubations contained capillaries equivalent to approximately 0.1 mg protein (mg_p). Age given in years; F = female, M = male.

Vivarium. A single intravenous injection was performed in a femoral vein of 1.8 ml of 0.01 M Na_2HPO_4/0.15 M NaCl (PBS, pH = 7.4), containing 100 μCi (312 μg) of ^{3}H-mouse IgG_{2a} and 25 μCi (0.6 μg) of ^{125}I-MAb83-14 for RM1 or 50 μCi (1.0 μg) of ^{125}I-MAb83-14 for RM2. At 0.5, 1, 2, 5, 15, 30, 60, 120, and 180 minutes after injection, 1 ml of blood was withdrawn and replaced by an equal volume of normal saline (7 U/ml heparin). Erythrocytes were removed by centrifugation and 50 μL aliquots of plasma were counted for total radioactivity in triplicate using double isotope liquid scintillation counting of ^{3}H and ^{125}I, as described previously (5); 100 μL of plasma was precipitated with 10% TCA to determine the fraction of total plasma radioactivity that was precipitable by TCA. At 180 minutes after isotope injection, the animal was euthanized with either 100 mg/kg of sodium pentobarbital or 2 ml Eutha-6 (Western Medical Supply, Arcadia, CA) intravenously, and brain was removed, weighed, and solubilized for double isotope liquid scintillation counting. In RM1, peripheral tissues (liver, spleen, heart, small intestine, abdominal muscle, lung, renal cortex, and omental fat) were also removed and analyzed by double isotope (^{3}H, ^{125}I) liquid scintillation counting for computation of the organ volume of distribution (V_D). The V_D of the mouse IgG_{2a} is considered identical to the plasma volume (V_O) of the organ. The V_D was determined from the ratio of ^{125}I- or ^{3}H-disintegrations/min (DPM) per g organ divided by the DPM per μL of terminal plasma. The ^{3}H and ^{125}I counts/min (CPM) were converted to DPM by standard quench correction curves that accounted for ^{125}I-spill-over into the ^{3}H window of the Packard Tri-Carb liquid scintillation spectrometer. In addition, approximately 1 g of brain tissue was homogenized in cold physiological buffer for capillary depletion analysis using the method described previously (18). The capillary depletion technique fractionates the total brain homogenate into the vascular pellet and the postvascular supernatant. The V_D values for the homogenate, postvascular supernatant, and vascular pellet were each expressed as μL per g brain.

Pharmacokinetic parameters were calculated by fitting plasma TCA-precipitable ^{3}H or ^{125}I radioactivity data to a bi-exponential equation, i.e.,

$$A(t) = A_1 e^{-K_1 t} + A_2 e^{-K_2 t}$$

where A(t) = % ID/ml of plasma radioactivity, and ID = injected dose. Plasma data were fit to the bi-exponential equation using a derivative-free non-linear regression analysis, PARBMDP (Biomedical Computer P-Series developed at the UCLA Health Sciences Computing Facilities). The data were weighted using weight = 1/(concentration)^2, where concentration = % ID/ml. The brain volume of distribution (V_D) of ^{125}I-MAb83-14 at 3 hours after i.v. injection was determined from the ratio of dpm/g tissue ÷ dpm/μL terminal plasma. Brain plasma volume of distribution (V_O) was determined by computation of the volume of distribution of the ^{3}H-mouse IgG_{2a} isotype control. The plasma clearance (Cl_{SS}), the steady state volume of distribution (V_{SS}), the mean residence time (MRT), the area under the plasma concentration curve (AUC), and the area under the moment curve (AUMC) were calculated from the pharmacokinetic parameters as follows (19):

$$\int_0^\infty AUC = \frac{A_1}{K_1} + \frac{A_2}{K_2}$$

$$\int_0^\infty AUMC = \frac{A_1}{K_1^2} + \frac{A_2}{K_2^2}$$

$$Cl_{SS} = \frac{D}{AUC}$$

$$V_{SS} = \frac{D \times AUMC}{AUC^2}$$

$$MRT = \frac{AUMC}{AUC}$$

where D = injected dose. The BBB permeability surface area (PS) product in brain was determined as follows:

$$PS = \frac{[V_D - V_0]C_p(T)}{\int_0^t AUC}$$

where Cp(T) = terminal plasma concentration. The brain delivery or % injected dose (ID)/g brain, at a given time (t) after i.v. injection is,

$$\frac{\%\ ID}{g} = PS \times \int_0^t AUC$$

$$\int_0^t AUC = \frac{A_1(1 - e^{-k_1 t})}{k_1} + \frac{A_2(1 - e^{-k_2 t})}{k_2}$$

The calculation of the PS product assumes there is no significant efflux of MAb from brain to blood during the experimental time period, e.g., 180 minutes.

Avidin-Biotin Immunocytochemistry

The reactivity of MAb83-7, MAb83-14, mouse IgG1 (the isotype control of MAb83-7) or mouse IgG_{2a} (the isotype control for MAb83-14) was assayed with the avidin-biotin immunoperoxidase technique described previously (20). Frozen Rhesus monkey or squirrel monkey brain cortex was thawed to −20°C, dipped in OCT at room temperature, and 4-6 μ sections were cut on a cryostat at −15°C. Sections were warmed to room temperature until air-dry, fixed in acetone at −20°C for 10 minutes, washed in PBS, air-dried and stored at −70°C. On the day of the assay, the slides were warmed to room temperature, washed in PBS, quenched with 0.1% H_2O_2 in PBS for 5-10 minutes, blocked with horse serum and stained with 2 μg/slide of immunoglobulin for 120 minutes at room temperature, followed by reaction with biotinylated horse anti-mouse immunoglobulin and stained with 3-amino-9-ethylcarbazole for 15 minutes. The sections were not counterstained, and were subsequently photographed. No specific immunostaining of cortical microvessels in squirrel monkey brain was observed with either MAb83-7 or MAb83-14.

RESULTS

Both MAb83-7 and MAb83-14 bind equally well to the

brain capillary endothelium of Rhesus monkey brain based on avidin-biotin immunocytochemistry (Figures 1A and 1B). The isotype controls for MAb83-7 (mouse IgG1) or MAb83-14 (mouse IgG_{2a}) do not immunostain brain microvessels (Figures 1C and 1D). MAb83-7 and MAb83-14 stained microvessels in both white matter and cortical gray matter. The number of vessels immunoreactive with MAb83-14 in white matter and gray matter was determined with an ocular micrometer and was 55 ± 4 and 234 ± 13 vessels per mm^2 (mean ± S.E., n = 9-11 fields), respectively.

Since the initial immunocytochemical evaluation showed both MAb83-7 and MAb83-14 strongly bound to the primate brain capillary insulin receptor, further analyses were performed with ^{123}I-labeled MAb83-14 or ^{125}I-labeled MAb83-7 using isolated autopsy human brain capillaries. ^{125}I-MAb83-14 strongly bound to the human brain capillaries (Figure 2). This binding was suppressed to background with high concentrations (80 μg/ml) of either MAb83-14 or MAb83-7 but not the isotype controls, mouse IgG1 or mouse IgG_{2a}. High concentrations (10 μg/ml) of porcine insulin inhibited the binding of ^{125}I-MAb83-14 by approximately 35%. The time course of ^{125}I-MAb83-14 or ^{125}I-MAb83-7 binding to human brain capillaries is shown in Figure 3. These studies demonstrate markedly different binding kinetics of the two monoclonal antibodies to human brain capillaries, as MAb83-14 bound to the capillary approximately 10-fold greater than MAb83-7. Approximately 70% of the MAb83-14 bound to the human brain capillary was endocytosed into a space that was resistant to a mild acid wash (Figure 3). The MAb is not significantly metabolized by the human brain capillaries. After two-hour incubations at 37°C, the medium TCA precipitability of the radiolabeled monoclonal antibodies was 95 ± 1% for MAb83-7 and 96 ± 1% for MAb83-14. The high binding of ^{125}I-MAb83-14 to the human brain microvessels used in the studies of Figures 2-3 was replicated with microvessels isolated from 2 other human autopsy brains, and the binding time course at 37°C for the 3 different sets of human brain capillaries (designated H1, H2, and H3) is shown in Table 1. The binding data in Table 1 are normalized by dividing the ^{125}I-MAb83-14 % bound by the mg protein of isolated capillaries (Methods). The binding data in Figures 2-5 used capillaries isolated from subject H2 (Table 1).

The saturability of ^{125}I-MAb83-14 binding was examined by varying the concentration of unlabeled MAb83-14, and a concentration of 0.09 μg/ml (0.60 nM) of MAb83-14 caused 50% displacement in the binding curve (Figure 4A). Scatchard analysis of the binding data (Figure 4B) showed that the K_D of MAb83-14 binding to the human insulin receptor was 0.45 ± 0.10 nM, and the binding B_{max} was 0.50 ± 0.11 $pmol/mg_p$.

The effect of increasing concentrations of MAb83-14 or

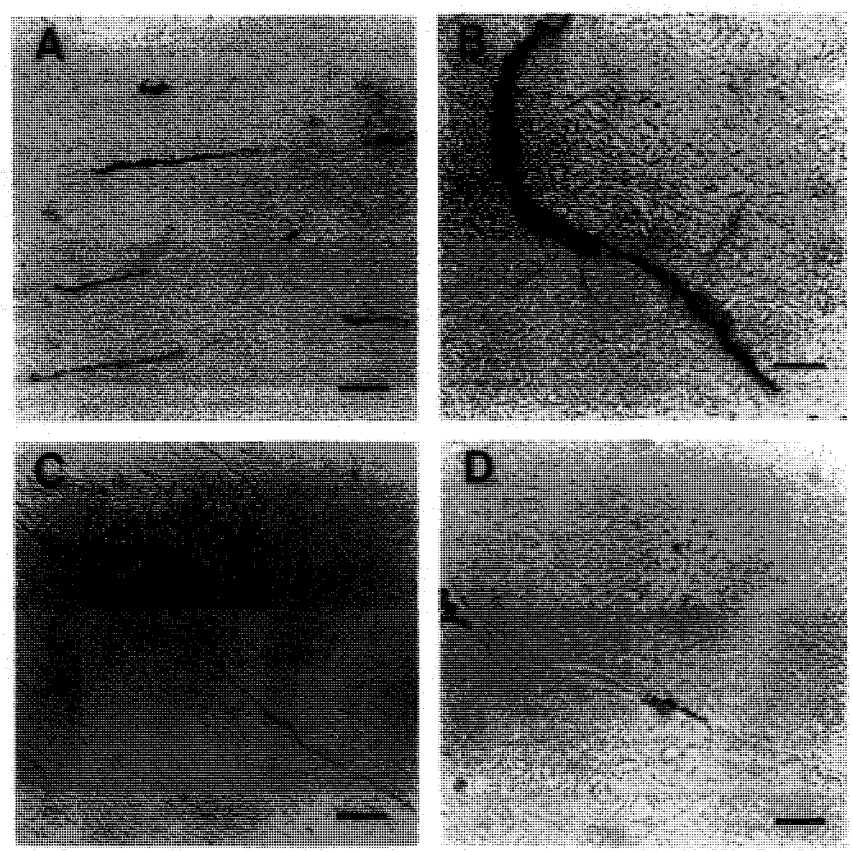

Fig. 1. Avidin-biotin immunocytochemistry of cryostat sections of rhesus monkey brain using 2 μg/slide of either MAb or isotype control. (A) MAb83-7. (B) MAb83-14. (C) Mouse IgG1, which is the isotype control for MAb83-7. (D) Mouse IgG_{2a}, which is the isotype control for MAb83-14. Magnification bars are 11 μ in B and D, and 28 μ in A and C.

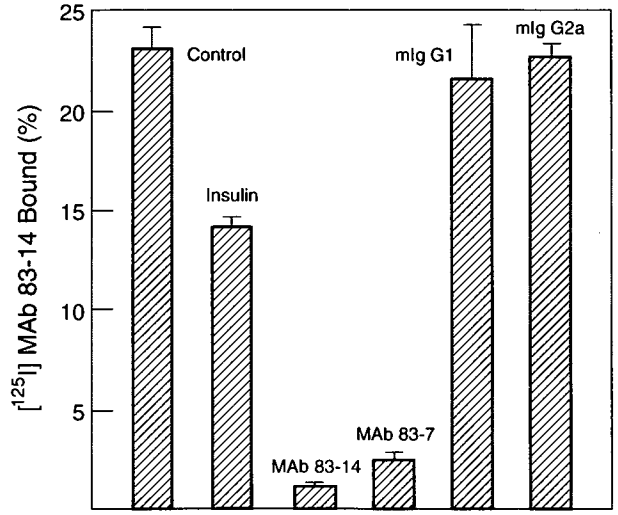

Fig. 2. Binding of ^{125}I-MAb83-14 to human brain capillaries. Incubations were performed at 37°C for 60 minutes in the presence of human capillaries equivalent to 140 μg of protein. MAb83-14, MAb83-7, mouse IgG1 or mouse IgG_{2a} were present in concentrations of 80 μg/ml (0.5 μM) and porcine insulin was present in a concentration of 10 μg/ml (2 μM). The % bound was less than 0.15% for all incubations when isolated capillaries were omitted from the incubation medium. Data are mean ± SE (n = 3).

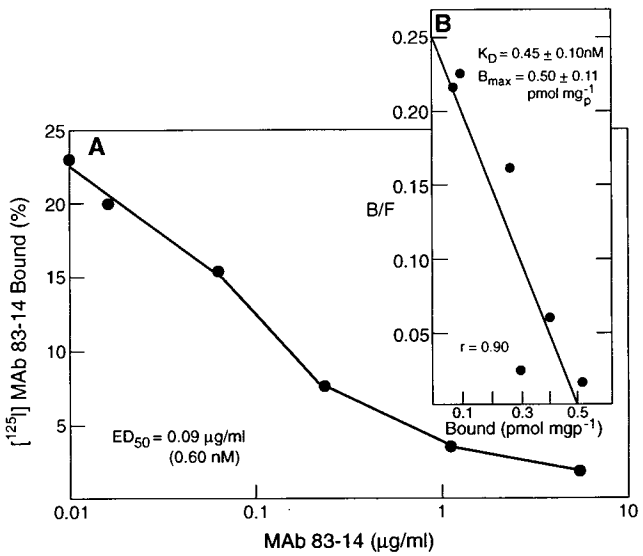

Fig. 4. (A) Binding of ^{125}I-MAb83-14 to isolated human brain capillaries is plotted vs. the concentration of MAb83-14 in the incubation medium. Incubations were carried out at 37°C for 60 minutes, and contained human brain capillaries equivalent to 100 μg protein. The 50% displacement (ED_{50}) of ^{125}I-MAb83-14 was observed at an MAb83-14 concentration of 0.09 μg/ml (0.60 nM). (B) Scatchard analysis of the binding data in panel A. The bound/free of B/F ratio is plotted vs. the bound (pmol/mg_p) MAb83-14. The dissociation constant K_D and the maximal binding (B_{max}) were determined from nonlinear regression analysis of the saturation data, as described previously (12).

mouse IgG_{2a} on ^{125}I-insulin binding to human brain capillaries is shown in Figure 5. Approximately 2/3 of the labeled insulin bound to the capillary was endocytosed, as represented by the portion of insulin binding that is non-saturable (dashed horizontal line, Figure 5); previous studies have shown that the non-saturable insulin binding corresponds to endocytosed insulin (12).

The pharmacokinetics and brain uptake of ^{125}I-MAb83-14 (also designated HIRMAb) was examined in two anesthetized Rhesus monkeys (RM1, RM2). The serum concentrations of either ^{125}I-HIRMAb or ^{3}H-mouse IgG_{2a} in the plasma compartment of the monkey was measured for up to 3 hours after a single intravenous injection, and these data are shown in Figure 6 for RM1. The serum profile for either RM1 or RM2 was subjected to a pharmacokinetic analysis, and the parameters are shown in Table 2. Both immunoglobulins have a half-time of distribution ($t^1_{1/2}$) of approximately 2 minutes, but the half-time of elimination ($t^2_{1/2}$) of the HIRMAb was 6- to 12-fold shorter than the half-time of elimination of the mouse IgG_{2a} isotype control (Table 2). The V_{SS} of the mouse IgG_{2a} isotype control, 52.9 ml/kg, is equivalent

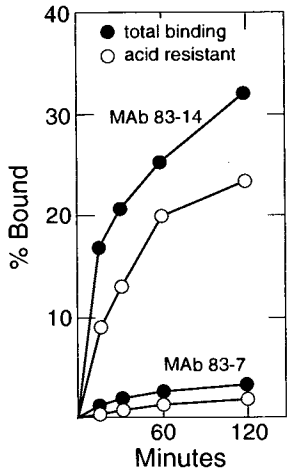

Fig. 3. The % binding of either ^{125}I-MAb83-14 of ^{125}I-MAb83-7 to isolated human brain capillaries at 37°C is plotted vs. time of incubation. Each incubation tube contained human brain capillaries equivalent to 140 μg of protein. Both total binding (closed circles) and binding resistant to a mild acid wash (open circles) are shown. Data are means of duplicates that varied less than 10%.

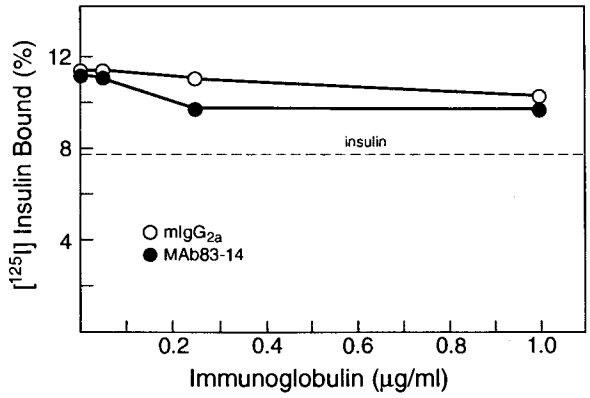

Fig. 5. The binding of ^{125}I-insulin to human brain capillaries is plotted vs. the medium concentration of either MAb83-14 or mouse IgG_{2a}. The dashed horizontal line shows the binding in the presence of 10 μg/ml insulin; this non-saturable binding represents endocytosed insulin (12). Data are means of duplicates that varied less than 10%.

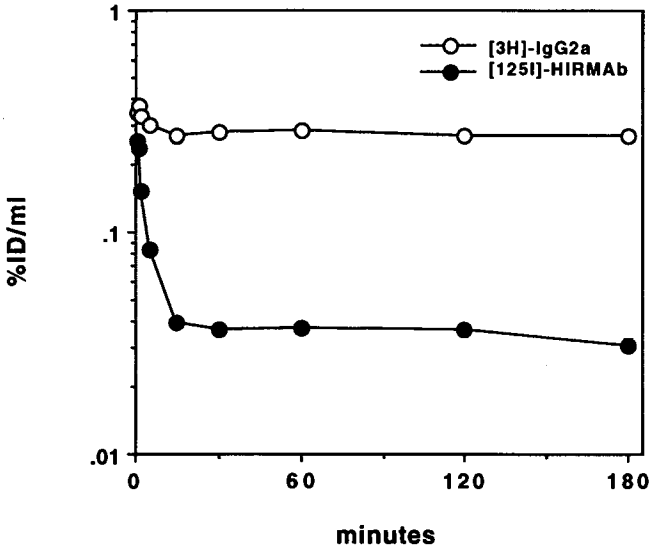

Fig. 6. The % injected dose (ID) per ml plasma of either ^{3}H-mouse IgG_{2a} isotype control (open circles) or ^{125}I-HIRMAb (closed circles) is plotted vs. time after single intravenous injection of the isotopes into an anesthetized rhesus monkey (RM1). Data are means of triplicates that varied less than 10%. The data shown were corrected by multiplying the total ^{3}H- or ^{125}I-dpm/ml by the fractional TCA precipitability. The TCA precipitability of the ^{3}H-mouse IgG_{2a} isotype control was greater than 99% at all time points. The TCA precipitability for the ^{125}I-HIRMAb was 99%, 98%, 94%, 94%, and 93% at 5, 15, 30, 120, and 180 minutes after injection, respectively. HIRMAb is MAb83-14.

to the plasma volume, whereas the V_{SS} of the HIRMAb, 367-406 ml/kg, was 7-fold greater than the V_{SS} of the mouse IgG_{2a}. The systemic clearance of the HIRMAb, 0.39-1.00 ml/min/kg, was 39- to 101-fold greater than the systemic clearance of the mouse IgG_{2a} isotype control (Table 2). The mean residence time of the HIRMAb was reduced to 7-16 hours, in comparison to the MRT of the mouse IgG_{2a} isotype control, which was 3.7 days (Table 2). The pharmacokinetics of plasma clearance of HIRMAb was similar in RM1 and RM2 as reflected by the comparable parameter estimates (Table 2).

The volume of distribution of the mouse IgG_{2a} isotype control and the HIRMAb in brain at 3 hours after a single intravenous injection of isotope was measured for neocortical gray matter, white matter, and choroid plexus, and these data are shown in Table 3 for both RM1 and RM2. The availability of these volume of distribution data, in conjunction with the 3-hour plasma AUC (Table 2), allowed for the computation of the BBB PS product. The PS products, and the

Table 2. Pharmacokinetic Parameters[a]

Parameter	Immunoglobulin		
	$mIgG_{2a}$	HIRMAb	
monkey	RM1	RM1	RM2
body weight (kg)	6.8	6.8	8.0
K_1 (min^{-1})	0.26	0.27	0.29
K_2 (hr^{-1})	0.011	0.060	0.14
$t_{1/2}^{1}$ (min)	2.7	1.9	2.4
$t_{1/2}^{1}$ (hr)	62.2	11.2	5.0
A_1 (% ID/ml)	0.091	0.27	0.21
A_2 (% ID/ml)	0.28	0.038	0.027
AUC^{180} (% ID · min/ml)	49.5	7.1	4.7
V_{ss} (ml/kg)	52.9	367	406
Cl_{ss} (ml/min/kg)	0.0099	0.39	1.00
MRT (hr)	89.8	15.9	6.8
AUC^{ss} (% ID · min/ml)	1497	38.1	12.5

[a] The plasma data for RM1 are shown in Figure 6. HIRMAb is MAb83-14; $AUC^{ss} = AUC \mid_{0}^{\infty}$; $AUC^{180} = AUC \mid_{0}^{180}$.

brain delivery (% injected dose per 100 g brain) of the HIRMAb for neocortex, white matter, or choroid plexus at 3 hours after injection, are shown in Table 3. The ^{125}I-HIRMAb was relatively metabolically stable as the %TCA precipitation in plasma was $\geq$ 93% for up to 3 hours after injection (Figure 6).

The capillary depletion technique was used to demonstrate transcytosis of the HIRMAb through the primate BBB, and these data are shown in Table 4 for brain tissue that was comprised of either mixed white and gray matter (RM1) or separated gray and white matter (RM2). The homogenate V_D value of the HIRMAb, 656 ± 132 μL/g, was intermediate between the V_D of neocortex and white matter in RM1 (Tables 3-4). Although there was enrichment of the HIRMAb in the vascular pellet, the V_D of the HIRMAb in the postvascular supernatant was 14- to 33-fold greater than the V_D of the mouse IgG_{2a} isotype control in the postvascular supernatant (Table 4), indicating rapid transcytosis of the HIRMAb through the primate BBB in vivo.

The V_D of the HIRMAb and the V_O of the mouse IgG_{2a} control antibody in peripheral organs were also measured at 180 minutes after intravenous injection in RM1 (Table 5). Consistent with the widespread distribution of the insulin receptor, the V_D value of the HIRMAb was 5- to 21-fold greater than the V_O of the mouse IgG_{2a} in peripheral tissues (Table 5). In contrast, the ratio of the HIRMAb V_D to the mouse IgG_{2a} V_O in brain neocortex was 42 for RM1 (Table 3).

Table 3. Brain Uptake Parameters for ^{125}I-MAb83-14 (HIRMAb)[a]

Organ	V_0 (μL/g)	V_D (μL/g)		PS (μL/min/g)		%ID/100 g tissue	
		RM1	RM2	RM1	RM2	RM1	RM2
neocortex	30 ± 2	1263 ± 129	1329 ± 80	5.4 ± 0.6	5.3 ± 0.3	3.8 ± 0.4	2.5 ± 0.1
white matter	31 ± 10	498 ± 141	508 ± 57	2.1 ± 0.6	1.9 ± 0.2	1.4 ± 0.4	0.90 ± 0.11
choroid plexus	139 ± 9	687 ± 96	3913 ± 122	2.4 ± 0.4	15.1 ± 0.5	1.7 ± 0.3	7.1 ± 0.2

[a] Mean ± S.E. (n = 3). The plasma volume of brain (V_0) was equal to the organ volume of distribution of the ^{3}H-mouse IgG_{2a}. RM1 = rhesus monkey 1; RM2 = rhesus monkey 2. Data obtained 3 hours after injection.

Table 4. Capillary Depletion Analysis of Brain Uptake of ^{125}I-MAb83-14 (HIRMAb)[a]

Monkey	Brain region	V_D (μL/g) Homogenate	Post-vascular supernatant	Vascular pellet
RM1	mixed gray/white	656 ± 132	231 ± 65	384 ± 31
RM2	gray matter	1572 ± 86	524 ± 57	657 ± 60
	white matter	615 ± 35	282 ± 4	173 ± 41

[a] Mean ± S.E. (n =). Plasma volume or V_0 = 18 ± 4, 16 ± 1, and 1.1 ± 0.4 μL/g for homogenate, post-vascular supernatant, and vascular pellet, respectively, as determined with ^{3}H-mouse IgG_{2a}. Data obtained at 3 hours after injection.

DISCUSSION

The findings of the present study are consistent with the following conclusions. First, MAb83-14 avidly binds human and old world monkey brain capillary (Figures 1, 2), and this binding is associated with endocytosis by the capillary (Figure 3). Second, the binding of MAb83-14 is much greater than the binding of MAb83-7 (Figure 3), and the high binding of MAb83-14 is associated with the high affinity of this MAb for the human BBB receptor (Figure 4). Third, MAb83-14 undergoes rapid binding and transcytosis through the Rhesus monkey BBB in vivo (Table 3-4), and has a BBB PS product several-fold higher than any known BBB transport vector. Fourth, the in vivo pharmacokinetic profile of MAb83-14 is favorable with a high V_{SS} and Cl_{SS} and a mean residence time of 7-16 hours (Table 2). The prolonged mean residence time is caused by stable plasma concentration following an initial phase of rapid tissue clearance of MAb83-14; this rapid clearance phase is completed within the first 15 minutes after intravenous injection (Figure 6). The present studies report on transport measurements in two monkeys (Tables 2-4). The results are highly consistent in both Rhesus monkeys, as the PS estimates for MAb83-14 are virtually identical in both RM1 and RM2 (Table 3).

MAb83-7 and MAb83-14 selectively bind the human, but not the rodent insulin receptor (21). The immunocytochemical studies shown in Figure 1 demonstrate that these monoclonal antibodies also bind to the insulin receptor of an old world primate such as the Rhesus monkey. In contrast, there was no measurable binding of either monoclonal antibody to capillaries of squirrel monkey brain (Methods), indicating a lack of cross-reactivity with the new world primate insulin receptor. This is consistent with the greater genetic similarity between humans and old world rather than new world primates (22). The continuous immunocytochemical staining of brain capillaries shown in Figure 1A and 1B indicates the site of the microvessel binding is the endothelial cell. The other cell which comprises the brain microcirculation is the pericyte, and pericyte immunostaining is a discontinuous pattern (23). In addition to Rhesus monkey brain capillaries (Figure 1), MAb83-14 avidly binds human brain capillaries (Table 1, Figure 2), and this binding is associated with endocytosis into a capillary space that is resistant to a mild acid wash (Figure 3). The rapid endocytosis of MAb83-14 is consistent with previous electron microscopic autoradiography studies demonstrating internalization of this monoclonal antibody into cells subsequent to binding to the plasma membrane insulin receptor (24). The evidence that the MAb83-14 binding site on the brain capillary is the insulin receptor is the partial, but reciprocal inhibition of binding by insulin or MAb83-14 (Figures 2, 5).

The higher binding of MAb83-14 to human brain capillaries relative to MAb83-7 (Figure 3) was unexpected. For example, both antibodies strongly stain Rhesus monkey brain capillaries (Figure 1). In addition, both antibodies increase thymidine uptake by transfected 3T3 cells to a comparable degree (ED_{50} = 1-2 nM) (21), and both antibodies co-precipitate the human insulin receptor (15). The rapid binding of MAb83-14 to human brain capillaries is associated with the very high affinity of this binding reaction. Scatchard analysis indicates the K_D of the binding reaction is low, 0.45 ± 0.10 nM (Figure 4). The maximal binding (B_{max}), 0.50 ± 0.11 pmol/mg protein, is comparable to previous estimates of the B_{max} of the human brain capillary insulin receptor (2). This correlation is also evidence that the MAb83-14 binding site on brain capillary endothelium is the insulin receptor.

Table 5. Peripheral Organ Uptake of ^{125}I-MAb83-14 (HIRMAb) and ^{3}H-mouse IgG_{2a} in RM1[a]

Organ	Mouse IgG_{2a} V_0 (μL/g)	HIRMAb V_D (μL/g)	HIRMAb V_D / mouse IgG_{2a} V_0 ratio
liver	439 ± 54	9137 ± 348	21
spleen	382 ± 4	6845 ± 443	18
heart	143 ± 20	1426 ± 254	10
small intestine	306 ± 69	2793 ± 666	9
abdominal muscle	46 ± 8	377 ± 39	8
lung	213 ± 16	1264 ± 130	6
renal cortex	767 ± 182	3805 ± 1024	5
omental fat	25 ± 3	131 ± 12	5

[a] Mean ± S.E. (n = 3 replicates). V_0 and V_D measured 3 hours after intravenous injection.

The binding of MAb83-14 to human brain capillaries is inhibited by high concentrations of MAb83-7, although the epitopes of MAb83-7 and MAb83-14 are separated by more than 200 amino acids along the α-chain of the insulin receptor (14). The epitope for MAb83-7 lies within the cysteine-rich domain of the α-subunit within amino acids 191-297, and the MAb83-14 epitope resides in the near carboxyl terminal region between amino acids 469-592 (14). Since the epitopes of MAb83-7 and MAb83-14 are spatially separated, the inhibition of ^{125}I-MAb83-14 binding to human brain microvessels by high concentrations (80 μg/mL or 0.5 μM) of MAb83-7 (Figure 2) suggests that MAb83-7 binding to the insulin receptor may induce conformational changes around the MAb83-14 binding site. The binding of MAb83-14 to the human brain capillary is relatively insensitive to insulin as a high concentration of insulin (2 μM) causes only a 30% reduction in the binding of MAb83-14 to human brain capillaries (Figure 2). The relative insensitivity to insulin of MAb83-14 receptor binding is consistent with recent studies showing that amino acids 485-599 of the α-subunit of the insulin receptor are not critical for receptor binding (25). Other investigations provide evidence that the insulin binding domain is near residues 704-718 of the carboxyl terminus of the α-subunit (26).

The high affinity binding of MAb83-14 to the human BBB insulin receptor facilitates passage of this monoclonal antibody through the BBB transcytotic pathway. Previous studies have demonstrated that the transcytosis of insulin through the BBB occurs via the brain capillary endothelial insulin receptor. The evidence for this is twofold. First, the transcytosis of insulin through the BBB in vivo is saturable (13). Second, there is only one saturable binding site for insulin on the brain capillary, and the molecular weight of this saturable binding site is identical to that of the α-subunit of the insulin receptor (12). The transcytosis of molecules through the capillary endothelium requires electron microscopic confirmation (27). The term transcytosis is applied to BBB transport because there is no paracellular endothelial pathway in brain (1). The transcytosis of molecules through the BBB may be quantified with autoradiography (13) or the capillary depletion technique (18). The latter method was used to document transcytosis of MAb83-14 through the Rhesus monkey BBB in vivo. As shown in Table 4, approximately 40% of the brain V_D of MAb83-14 is contributed by antibody distribution into the postvascular supernatant, which represents transcytosed antibody. Approximately 60% of the total volume of distribution in brain is contributed by the vascular pellet. The latter compartment represents MAb83-14 still residing within the brain capillary endothelium awaiting further passage through the transcytotic compartment. The volumes of distribution shown in Table 4 for RM1 were determined from samples comprised of both white and gray matter, and the V_D for the total homogenate (Table 4) is intermediate between the V_D value for neocortical gray matter and white matter for RM1 (Table 3). The distribution of MAb83-14 into gray matter is approximately 2½-fold greater than for white matter (Tables 3-4). This enrichment in brain uptake of MAb83-14 in gray vs. white matter parallels the greater microvascular density in gray matter vs. white matter (28), and parallels the density of vessels in rhesus monkey gray matter and white matter that are immunoreactive with MAb83-14 (Results).

The high uptake of MAb83-14 by choroid plexus is consistent with previous studies demonstrating insulin receptor in this tissue (27,29). The density of the insulin receptor in choroid plexus is much greater than the receptor density in brain parenchyma (29). The finding that the MAb83-14 V_D in neocortex is comparable to the V_D of the antibody in choroid plexus underscores the very high density of insulin receptor in primate brain endothelial cells. This high density is also found in human brain capillaries. The binding of MAb83-14 to human brain capillaries shown in Figure 3 is approximately 300%/mg protein at 2 hours of incubation (Table 1), and this binding is severalfold greater than the binding of other ligands to human brain microvessels reported in previous studies (2). The insulin receptor on choroid plexus epithelium may mediate the selective transport of circulating insulin into cerebrospinal fluid (CSF) (30). The contribution of choroidal transport of MAb83-14 to overall brain uptake of the circulating antibody is small compared to BBB transport, owing to the vastly greater surface area of the BBB compared to choroid plexus epithelium (2).

The active binding of MAb83-14 to human brain capillaries (Figures 2-4) is paralleled by the high permeability of the Rhesus monkey BBB to this monoclonal antibody. BBB permeability is quantified by determination of the PS product, and the PS value for MAb83-14 is 2-5 μL/min•g for the primate BBB (Table 3). This PS value is higher than the BBB PS value for insulin in the rat brain, which is 1 μL/min•g (31), indicating the BBB insulin receptor transcytosis system is more active in primates than in rats. The plasma volume (V_O) in the primate brain, 18-30 μL/g (Tables 3-4) is also higher than in the rat brain (31), and may reflect a greater vascular density in the primate brain relative to the rat brain. However, the V_O is included in the PS computation (Methods); therefore, the higher primate V_O does not contribute to the elevated PS value for MAb83-14 estimated for the primate BBB. The high magnitude of the PS product in the primate is illustrated by comparing the BBB PS product for MAb83-14 in the primate brain (Table 3) with previous measurements of BBB PS product for the OX26 monoclonal antibody in the rat brain. The BBB PS product of the OX26 monoclonal antibody in the rat at 1, 2, and 3 hours after injection may be calculated from previously reported data (5), and is 1.56, 1.08, and 0.65 μL/min/g, respectively. The time-dependent decrease in the PS product reflects egress of the antibody from brain subsequent to uptake (32). The time-dependency of the BBB PS product in the Rhesus monkey could not be determined due to the limited availability of the primate. Comparison of the 3-hour BBB PS product for the OX26 monoclonal antibody in the rat and the BBB PS product for MAb83-14 in the Rhesus monkey shows that the PS product for MAb83-14, 5.4 μL/min/g (Table 3), is 8-fold higher than the PS product for the OX26 monoclonal antibody.

The delivery of MAb83-14 to the brain is a function not only of the BBB PS product, but also of the plasma AUC (32). The % injected dose of the antibody delivered per 100 g brain (Table 3) is in direct proportion to both the PS product and the plasma AUC (Methods). Despite the high Cl_{SS}

and V_{SS} of MAb83-14 in the Rhesus monkey (Table 1), the plasma AUC is within the range that allows for substantial brain delivery of MAb83-14. For example, 3-4% of the injected dose of MAb83-14 is delivered to 100 g of primate brain (Table 3); 100 g is equal to the weight of the brain in the Rhesus monkey (33). The high plasma AUC of MAb83-14 is due to the stable plasma concentration of this antibody, following an initial rapid uptake of the antibody during the first 15 minutes after injection (Figure 6). Insulin receptor is distributed in peripheral tissues and MAb83-14 rapidly distributes to liver and spleen of the Rhesus monkey (Table 5). However, this rapid uptake into peripheral tissues equilibrates during the first 15 minutes after intravenous injection, and this equilibration allows for a stable plasma concentration of the antibody (Figure 6). Similar observations have been made previously with the OX26 monoclonal antibody, wherein it was demonstrated that the rapid uptake of the antibody by liver reaches equilibration within the first 15-30 minutes after administration in the rat (5). This equilibration of liver uptake sites allows for stabilization of the plasma concentration, for maintenance of a high plasma AUC, and for significant brain delivery of the monoclonal antibody.

The relative distribution of HIRMAb into brain and peripheral tissues also has pharmacokinetic implications for brain delivery when the MAb is administered at high systemic doses. At high plasma concentrations of MAb, the BBB receptor site is saturated resulting in a reduction in the BBB PS product (34). However, under these conditions the peripheral receptor also becomes saturated and this increases the plasma AUC. The decreased PS and increased AUC result in minimal changes in brain delivery at high antibody doses (34). High concentrations of MAb83-14 may also inhibit insulin binding to the insulin receptor (21). However, the binding of insulin to the BBB insulin receptor is relatively insensitive to concentrations of MAb83-14 less than 1 μg/mL (Figure 5), which is equivalent to an MAb83-14 concentration of 6 nM. Higher concentrations of MAb83-14 have been shown to further inhibit insulin binding to the insulin receptor (21).

In summary, the present studies demonstrate very active binding of MAb83-14 to isolated human brain capillaries. This binding is associated with rapid transcytosis across the BBB in the Rhesus monkey in vivo. These results suggest that the high degrees of brain delivery may be achieved with monoclonal antibodies that bind with high affinity to BBB surface membrane receptors.

ACKNOWLEDGMENTS

Emily Yu skillfully prepared the manuscript. Supported by NIH grant RO1-DA06748. The authors are indebted to Dr. Kenneth Siddle for providing the MAb83-14 and MAb83-7 ascites, to Dr. Lary Walker for providing the frozen Rhesus and squirrel monkey brain specimens, and to Dr. Harry Vinters for providing the human autopsy brain.

REFERENCES

1. Brightman, M. W. Morphology of blood-brain interfaces. *Exp. Eye Res.* 25: 1-25, (1977).
2. Pardridge, W. M. *Peptide Drug Delivery to the Brain.* Raven Press/New York, 1-357, (1991).
3. Kumagai, A. K., J. Eisenberg, and W. M. Pardridge. Absorptive-mediated endocytosis of cationized albumin and a β-endorphin-cationized albumin chimeric peptide by isolated brain capillaries. Model system of blood-brain barrier transport. *J. Biol. Chem.* 262: 15214-15219, (1987).
4. Friden, P. M., L. R. Walus, G. F. Musso, M. A. Taylor, B. Malfroy, and R. M. Starzyk. Anti-transferrin receptor antibody and antibody-drug conjugates cross the blood-brain barrier. *Proc. Natl. Acad. Sci. USA* 88: 4771-4775, (1991).
5. Pardridge, W. M., J. L. Buciak, and P. M. Friden. Selective transport of anti-transferrin receptor antibody through the blood-brain barrier in vivo. *J. Pharmacol. Exp. Ther.* 259: 66-70, (1991).
6. Bickel, U., T. Yoshikawa, E. M. Landaw, K. F. Faull, and W. M. Pardridge. Pharmacologic effects in vivo in brain by vector-mediated peptide drug delivery. *Proc. Natl. Acad. Sci. USA* 90: 2618-2622, (1993).
7. Friden, P. M., L. R. Walus, P. Watson, S. R. Doctrow, J. W. Kozarich, C. Backman, H. Bergman, B. Hoffer, F. Bloom, and A-C. Granholm. Blood-brain barrier penetration and in vivo activity of an NGF conjugate. *Science* 259: 373-377, (1993).
8. Jefferies, W. A., M. R. Brandon, S. V. Hunt, A. F. WIlliams, K. C. Gatter, and D. Y. Mason. Transferrin receptor on endothelium of brain capillaries. *Nature* 312: 162-163, (1984).
9. Fishman, J. B., J. B. Rubin, J. V. Handrahan, J. R. Connor, and R. E. Fine. Receptor-mediated transcytosis of transferrin across the blood-brain barrier. *J. Neurosci. Res.* 18: 199-304, (1987).
10. Pardridge, W. M., J. Eisenberg, and J. Yang. Human blood-brain barrier transferrin receptor. *Metabolism* 36: 892-895, (1987).
11. Jefferies, W. A., M. R. Brandon, A. F. Williams, and S. V. Hunt. Analysis of lymphopoietic stem cells with a monoclonal antibody to the rat transferrin receptor. *Immunology* 54: 333-341, (1985).
12. Pardridge, W. M., J. Eisenberg, and J. Yang. Human blood-brain barrier insulin receptor. *J. Neurochem.* 44: 1771-1778, (1985).
13. Duffy, K. R., and W. M. Pardridge. Blood-brain barrier transcytosis of insulin in developing rabbits. *Brain Res.* 420: 32-38, (1987).
14. Prigent, S. A., K. K. Stanley, and K. Siddle. Identification of epitopes on the human insulin receptor reacting with rabbit polyclonal antisera and mouse monoclonal antibodies. *J. Biol. Chem.* 265: 9970-9977, (1990).
15. Soos, M. A., K. Siddle, M. D. Baron, J. M. Heward, J. P. Luzio, J. Bellatin, and E. S. Lennox. Monoclonal antibodies reacting with multiple epitopes on the human insulin receptor. *Biochem. J.* 235: 199-208, (1986).
16. Yoshikawa, T., and W. M. Pardridge. Biotin delivery to brain with a covalent conjugate of avidin and a monoclonal antibody to the transferrin receptor. *J. Pharmacol. Exp. Ther.* 263: 897-903, (1992).
17. Pardridge, W. M., J. L. Buciak, and T. Yoshikawa. Transport of recombinant CD4 through the rat blood-brain barrier. *J. Pharmacol. Exp. Ther.* 261: 1175-1180, (1992).
18. Triguero, D., J. B. Buciak, and W. M. Pardridge. Capillary depletion method for quantifying blood-brain barrier transcytosis of circulating peptides and plasma proteins. *J. Neurochem.* 54: 1882-1888, (1990).
19. Gibaldi, M. and D. Perrier. *Pharmacokinetics.* Marcel Dekker, Inc./New York, (1982).
20. Hsu, S., L. Raine, and H. Fanger. A comparative study of the peroxidase method and an avidin-biotin complex method for studying polypeptide hormone with radioimmunoassay antibodies. *Am. J. Clin. Pathol.* 75: 734-738, (1981).
21. Soos, M. A., R. M. O'Brien, N. P. J. Brindle, J. M. Stigter, A. K. Okamoto, J. Whittaker, and K. Siddle. Monoclonal antibodies to the insulin receptor mimic metabolic effects of insulin but do not stimulate receptor autophosphorylation in transfected NIH 3T3 fibroblasts. *Proc. Natl. Acad. Sci. USA* 86: 5217-5221, (1989).
22. Swindler, D. R., and J. Erwin, editors. *Comparative Primate*

Biology, vol. 1 (Systematics, Evolution, and Anatomy). Alan R. Liss, Inc./New York, (1986).
23. Pardridge, W. M., J. Yang, J. Buciak, and W. W. Tourtellotte. Human brain microvascular DR antigen. *J. Neurosci. Res.* 23: 337-341, (1989).
24. Paccaud, J. -P., K. Siddle, and J. -L. Carpentier. Internalization of the human insulin receptor. The insulin-dependent pathway. *J. Biol. Chem.* 267: 13101-13106, (1992).
25. Sung, C. K., K. Y. Wong, C. C. Yip, D. M. Hawley, and I. D. Goldfine. Deletion of residues 485-599 from the human insulin receptor abolishes antireceptor antibody binding and influences tyrosine kinase activation. *Molec. Endocrinol.* 8: 315-324, (1993).
26. Kurose, T., M. Pashmforoush, Y. Yoshimasa, R. Carroll, G. P. Schwartz, G. T. Burke, P. G. Katsoyannis, and D. F. Steiner. Cross-linking of a B25 azidophenylalanine insulin derivative to the carboxyl-terminal region of the α-subunit of the insulin receptor. *J. Biol. Chem.* 269: 29190-29197, (1994).
27. Vorbrodt, A. W., Dobrogowska, D. H., and Lossinsky, A. S. Ultrastructural study on the interaction of insulin-albumin-gold complex with mouse brain microvascular endothelial cells. *J. Neurocytol.* 201-208, (1994).
28. Lierse, W., and E. Horstmann. Quantitative anatomy of the cerebral vascular bed with especial emphasis on homogeneity and inhomogeneity in small parts of the gray and white matter. *Acta Neurol.* 14: 15-19, (1959).
29. Baskin, D. G., B. Brewitt, D. A. Davidson, E. Corp, T. Paquette, D. P. Filgewicz, T. K. Lewellen, M. K. Graham, S. G. Woods, and D. M. Dorsa. Quantitative autoradiographic evidence for insulin receptors in the choroid plexus of the rat brain. *Diabetes* 35: 246-249, (1986).
30. Woods, S. C., and D. Porte, Jr. Relationship between plasma and cerebrospinal fluid insulin levels in dogs. *Am. J. Physiol.* 233: E331-E334, (1977).
31. Poduslo, J. F., G. L. Curran, and C. T. Berg. Macromolecular permeability across the blood-nerve and blood-brain barriers. *Proc. Natl. Acad. Sci. USA* 91: 5705-5709, (1994).
32. Kang, Y. -S., and W. M. Pardridge. Use of neutral-avidin improves pharmacokinetics and brain delivery of biotin bound to an avidin-monoclonal antibody conjugate. *J. Pharmacol. Exp. Ther.* 269: 344-350, (1994).
33. Bourne, G. H. *The Rhesus Monkey*, Vol. 1 (Anatomy and Physiology). Academic Press/New York, 6-10, (1975).
34. Kang, Y. -S., U. Bickel, and W. M. Pardridge. Pharmacokinetics and saturable blood-brain barrier transport of biotin bound to a conjugate of avidin and a monoclonal antibody to the transferrin receptor. *Drug Metab. Disp.* 22: 99-105, (1994).